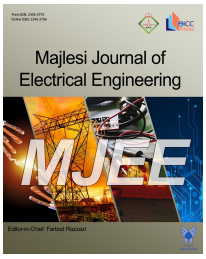

Volume 19, Issue 2, 192530 (1-9)

Majlesi Journal of Electrical Engineering (MJEE)

https://doi.org/10.57647/j.mjee.2025.1902.30

Synthesis and characterization of reduced graphene using vitamin C for conductive electrode applications

Zeng Feihu[1,2], SyYi Sim[3,*], Wang Zhiwen[1,2], Lai Mingrui[1]

[1]*Liming Vocational University, Quanzhou, China.*
[2]*Faculty of Engineering Technology, University Tun Hussein Onn Malaysia, Pagoh, Johor, Malaysia.*
[3]*Faculty of Electrical and Electronic Engineering, University Tun Hussein Onn Malaysia, Johor, Malaysia.*

[*]**Corresponding author:** sysim@uthm.edu.my

Original Research

Received:
23 March 2025
Revised:
15 April 2025
Accepted:
10 May 2025
Published online:
1 June 2025

Abstract:

In this study, reduced graphene oxide (rGO) was synthesized by reducing graphene oxide (GO) using Vitamin C (VC) as a reducing agent, to create a conductive electrode material. The structural and property effects of VC/GO mass ratios, reaction temperature and time on rGO were investigated in detail. Structural characterization and conductivity assessments of both GO and rGO were conducted using powder X-ray diffraction (XRD), Fourier-transform infrared (FTIR) spectroscopy, scanning electron microscopy (SEM), Brunauer-Emmett-Teller (BET) surface area analysis, and a four-probe conductivity tester. The results showed that VC as a reducing agent effectively reduces the functional groups on the GO surface, forming C=C bonds, while also increasing the d-spacing of rGO. The increase of reaction temperature promotes the ionization and decomposition of VC, thereby improving the reaction efficiency. The synthesized rGO exhibited a porous network with an irregular structure formed by interconnected, wrinkled nanosheets. Optimal conditions were observed when the VC/GO mass ratio was 1:1, the reaction temperature was 100 °C, and the reaction time was 3 hours. Under these conditions, the synthesized rGO material achieved a resistivity of 1.82 Ω·cm and a resistance value of 2.75 Ω, positioning it as an excellent electrode material.

Keywords: Vitamin C; Graphene; Reduced graphene oxide; Electrode

1. Introduction

Reduced graphene oxide (rGO), a derivative of graphene, has recently attracted significant attention due to its unique structure and excellent electrical conductivity, mechanical strength, and thermal conductivity [1]. rGO forms a graphene-like structure by combining small amounts of functional groups such as epoxy, carbonyl, and carboxyl groups through a layer-stacked carbon-hexadecane cyclic $\pi - \pi$ conjugated backbone. rGO finds a wide range of applications, especially in the fields of sensing, energy storage and photocatalysis [2]. The rGO-based sensors are capable of detecting chemically aggressive gases [3], and they can also be combined with carbon nanotubes to form sensors with fast response and good storage stability. In terms of energy storage, rGO, as an anode material for sodium-ion batteries, has demonstrated excellent sodium storage performance and cycling stability by modulating its microstructure [4], and it can also be combined with iron oxide nanoparticles to form a synergistic effect generated by the effective bonding of Fe-O-C, which improves the specific capacitance and cycling stability [5]. Moreover, rGO can also provide suitable growth templates for various metal oxide (MOs) nanoparticles and be utilized in the advanced electrode fabrication [6]. Therefore, the study of rGO synthesis is of great significance for the development of high-performance electrode materials.

Current methods for graphene production can be categorized into destruction and construction approaches [7], encompassing techniques such as mechanical exfoliation [8], chemical vapor deposition (CVD) [9], liquid-phase exfoliation [10], and chemical reduction [11]. The chemical reduction method for graphene is noted for its low cost and high efficiency. Graphite is used to prepare graphene oxide (GO), which can be uniformly dispersed in various solvents due to the -OH and -COOH groups on its surface, GO exists as monolayers of carbon sheets [12]. However, to achieve conductivity, it is necessary to overcome the inherent structural defects of GO by reducing and removing the -OH, -COOH, and other functional groups, thereby restoring the sp^2 structure. Research has shown that GO is

a solution-processable, non-stoichiometric macromolecule with approximately $2-3$ nm sp^2 clusters isolated by a sp^3 matrix. Its reduction leads to the formation of new sp^2 domains that connect with existing sp^2 clusters [13], thereby enhancing conductivity. Thus, using agents to reduce GO provides a pathway to produce high surface area, thin-layer graphene materials.

Currently, various substances can be used as reducing agents, including hydrazine hydrate [14], amino acids [15], urea [16], hydriodic acid [17], and sodium citrate. Although a wide range of reducing agents is available, research has focused on selecting environmentally friendly, safe, and readily available agents. Different reducing agents have varying effects on the reduction of GO to rGO. Vitamin C (VC), a water-soluble vitamin, contains an enediol structure that readily releases highly reductive hydrogen atoms in water. Compared to other reducing agents, VC has been found to yield highly reduced suspensions comparable to those provided by hydrazine [18]. Some researchers have utilized VC to reduce GO to produce rGO [19, 20], which has been used for in vitro detection of animal dopamine [21] and the removal of aflatoxin B1 and benzo(a)pyrene in vegetable oils [22]. Ferda [23] studied the different weight ratios of vitamin C: GO (1:1, 1.5:1 and 2:1) on the structural and thermal properties of rGO. Other studies have explored the influences of reaction temperatures (70, 90 and 100 °C) and heating times (30, 45 and 60 min) on the structure of rGO, but not its conductivity. Graphitic foil was also prepared by blade coating, hot-pressing, and graphitization process through solution-derived graphene oxide (GO), employing VC as a reductant and binder [24]. The tensile strength and thermal diffusivity of graphitic foil were investigated. However, the study of rGO system prepared from VC-reduced GO has not been reported.

This paper reports the use of vitamin C (VC) as a reductant to reduce GO synthesized using the improved Hummers method to produce rGO. The effects of the synthesis process, including the mass ratio of VC to GO, reaction time, and reaction temperature, on the structure of the prepared rGO are investigated in detail. The mechanism of VC reduction of GO is also discussed, and the resulting rGO demonstrates potential as an excellent electrode material.

2. Experimental

The preparation of rGO is described in detail, followed by a description of the characterization techniques used for the samples.

2.1 Material and chemicals

Flake graphite (100 mesh, 200 μm) was brought from Qingdao Dongkai Graphite Co., Ltd.Qing dao, China. All the chemicals were purchased from Sinopharm Chemical Reagent Co., Ltd.,China.

2.2 Reduced graphene oxide preparation

There are two steps in the process of rGO preparation, as shown in Fig. 1.

Step 1: The modified Hummer's method was used to prepare GO from graphite. Sulfuric acid (H_2SO_4, 21 mL) and graphite (1.0 g) were mixed in a beaker, adding potassium permanganate ($KMnO_4$, 3 g) and then stirring for 2 hours at less than 15 °C until the solution turned grey-green. Transfer the breaker into a 35 °C water bath for 0.5 h. Deionized (DI) water (46 mL) was added to prevent a dramatic increase in temperature, ensuring the system's temperature does not drop below 98 °C for 0.5 h. Once cooled to 60 °C, 30% hydrogen peroxide was added, and the mixture was allowed to react for 30 minutes. Finally, the solution was washed with hydrochloric acid (HCl, 10%) to remove the metal ions, followed by centrifugation with DI water until the pH of the solution was between 6 to 7. The resulting graphene oxide (GO) films were dried in an oven at 50 °C. The UV-visible absorption spectrum of the produced GO is shown in Fig. 2, which displays a characteristic absorption peak near 230 nm and a broad shoulder peak at 300 nm, These peaks are typical of GO, represented the $\pi-\pi^*$ of C=C and the n$-\pi^*$ electron transition of C=O in the GO conjugated system, respectively [25]. This confirms that the produced sample is indeed GO.

Step 2: A GO film (0.3 g) was mixed with 75 mL of deionized water and ultrasonicated for 10 minutes to disperse the GO in the aqueous solution. Vitamin C (VC) was then added at a specific ratio to the solution, and the reaction was carried out in a 100 mL reactor at different temperatures. The resulting samples were washed and centrifuged repeatedly with deionized water to remove residual VC and other by-products from the system. Finally, the rGO was obtained by vacuum freeze-drying.

2.3 Characterization techniques

A UV-visible spectrophotometer (UV-9000) was used to analyze the characteristic UV absorption of GO. Absorp-

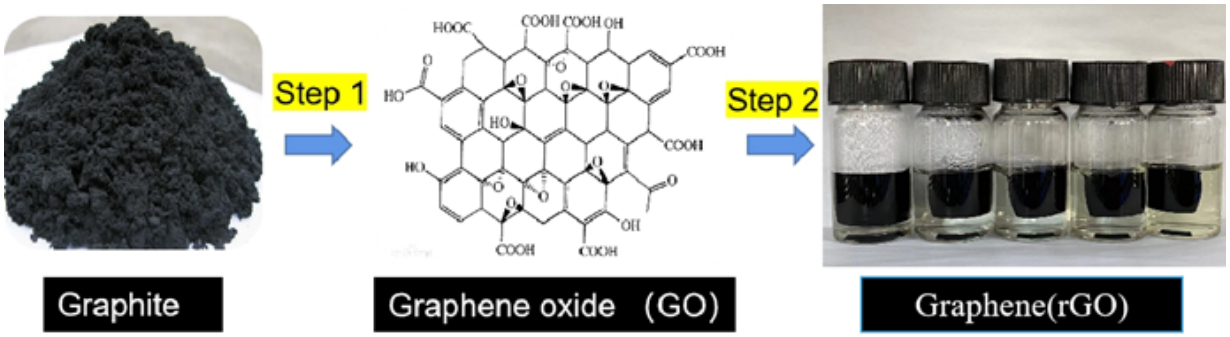

Figure 1. Process of rGO preparation.

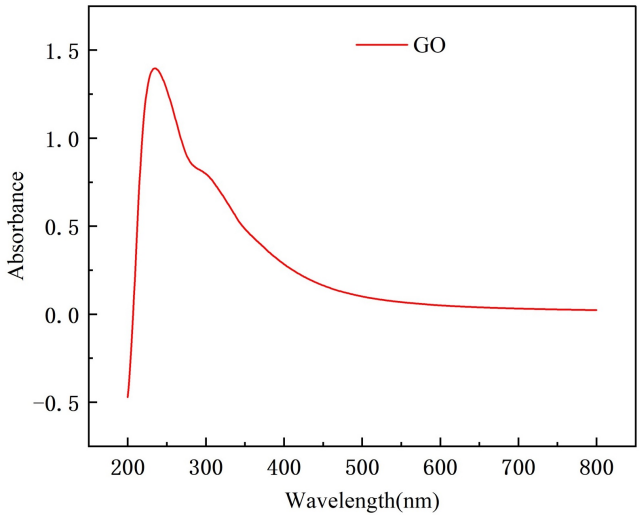

Figure 2. Ultraviolet-visible absorption spectra of graphene oxide.

tion data were recorded in the wavelength range of 200 to 800 nm. The morphological characteristics of both GO and rGO were obtained using a scanning electron microscope (SEM, Nova200, FEI) at an accelerating voltage of 10.0 kV. Structural changes from GO to rGO were investigated using X-ray diffraction (XRD) with a MiniFlex600 (Cu Kα X-ray of 0.154 nm wavelength, the voltage of 40 kV) over a θ range from 10° to 50°. Changes in chemical bonding and functional groups after successful reduction were examined by Fourier transform infrared spectroscopy (FTIR), with data recorded on an IRAffinity-1S. The specific surface area of the samples was determined through nitrogen adsorption measurements at 77 K using the linear part of the Brunauer-Emmett-Teller (BET) equation. The pore size distribution was evaluated according to the nonlocal density functional theory using a JW-BK200B device (Beijing Jingweigaobo Device Co., Ltd., Beijing, China). A ST2258C multifunctional digital four-probe tester (Jingge, Jiangsu, China) was used to analyze the resistivity (ρ) and resistance(R) of the samples.

2.4 Mechanism

VC molecule possesses a hyphenated dienol structure that readily releases hydrogen (H) atoms with strong reducing properties. This ability allows VC to react with the epoxy groups, carboxyl groups, carbonyl groups, and other structures present in GO, ultimately yielding reduced rGO. Gao [11] suggested that the reduction process may involve a combination of S_N2 nucleophilic substitution and thermal reduction reactions. In this mechanism, the five-membered ring in VC has the ability to absorb electrons, facilitating the separation of hydroxyl groups into H protons and alkoxide anions. These anions then attack the epoxy or hydroxyl group of GO, forming an intermediate that decomposes through thermal reactions to produce C=C bonds, as illustrated in Fig. 3.

3. Results and discussion

The main influencing factors for the preparation of rGO were examined, including the VC/GO Mass Ratios, reaction time and reaction temperature. The samples with the best conductivity were also characterized and analyzed.

3.1 Vitamin C/graphene oxidate mass ratios

Fig. 4 showed the effect of VC/GO mass ratios on the crystal structure and resistivity of rGO. X-ray diffraction (XRD) patterns were employed to analyze the crystallinity and interlayer distance. Fig. 4 (a) displayed the XRD patterns

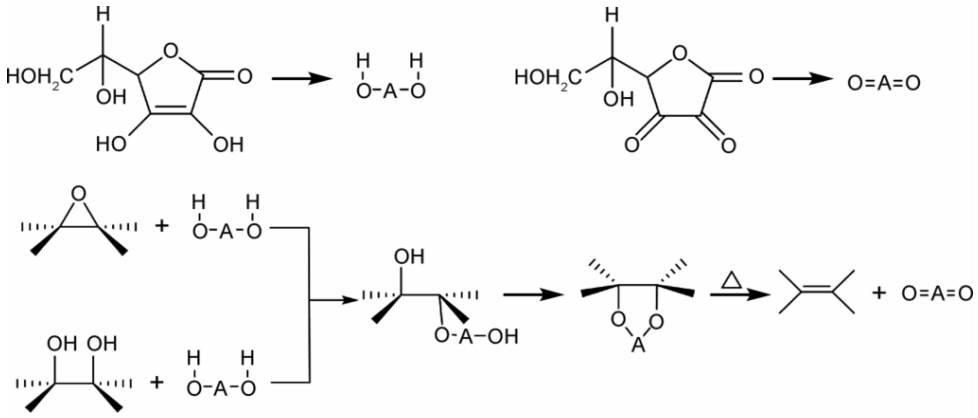

Figure 3. Vitamin C induced reduction mechanism [11].

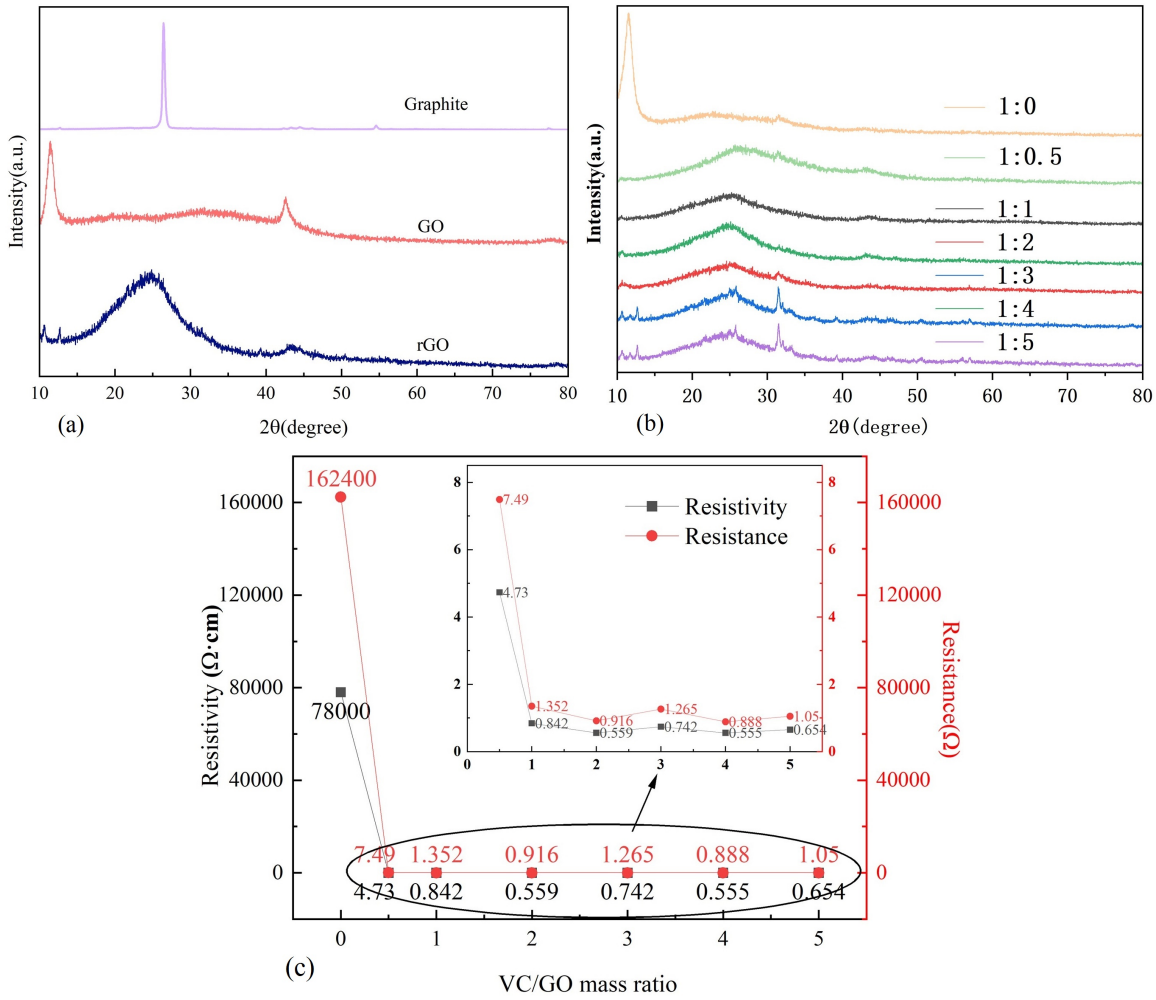

Figure 4. (a) (b)X-ray Diffraction (c) Conductivity of samples at different VC/GO mass ratios (Reaction condition: 100 °C, 4 h.).

of graphite, GO, and rGO used in this study. A typical diffraction peak for GO was observed at 11°, indicating an interlayer distance of 0.780 nm, surpassing that of graphite (d = 0.345 nm) and rGO (d = 0.361 nm). This expansion in interlayer spacing was attributed to the introduction of hydroxyl and epoxy functional groups between layers during the oxidation of graphite [26], consequently augmenting the interlayer distance and diminishing conductivity. Furthermore, the reduction of GO by VC to prepare rGO demonstrates that VC and its decomposition derivatives possess nucleophilic groups capable of opening the epoxy groups in GO. T Consequently, the diffraction peak at 11° disappeared, and peaks appeared in the range of 24°-27° and at 43.1°, corresponding to the (002) and (020) crystallographic planes of graphene, respectively [27].

The effects of VC/GO mass ratios on the rGO crystal structure were observed in Fig. 4 (b). Direct synthesis of rGO without the use of VC as a reducing agent failed to show the characteristic peaks of rGO, highlighting the crucial role of VC in transforming GO into rGO. When the VC/GO mass ratio reached 0.5, the typical peak at 11° disappeared, replaced by broad peaks that indicated the short-range order of the structure and the successful removal of oxygen-containing functional groups. The d-spacing value calculated by X-ray diffraction reduced from 0.764 nm to 0.344 nm, confirming that the oxidized functional groups were reduced and the layer spacing decreased as GO is reduced. Gao's study on the reduction of GO by VC revealed that GO initially contains four different chemical states of carbon: graphite C, C-O, C=O, and O-C=O. The study also demonstrated that while rGO retains these carbon states after reduction, the quantity of oxidized carbon in rGO was significantly lower compared to GO [20]. As the VC/GO mass ratio increased, a rapid decrease in resistivity was observed. However, beyond a VC/GO mass ratio of 1, additional VC does not further reduce resistivity. This phenomenon occurs because the excess VC adsorbed on the graphite surface was not completely removed by deionized water, forming a structure unfavourable to conductivity with the rGO. As shown in Fig. 4 (b), the increase in the amount of VC led to the appearance of many stray peaks in the X-ray diffraction pattern, supporting this conclusion. The d-spacing of rGO increased from 0.344 nm (VC/GO = 1:0.5) to 0.361 nm (VC/GO = 1:5), indicating that the excess VC formed the P-P stacking between the rGO layers and thereby preventing the agglomeration.

3.2 Reaction time

The XRD patterns and conductivity of samples synthesized at different reaction times were illustrated in Fig. 5. In

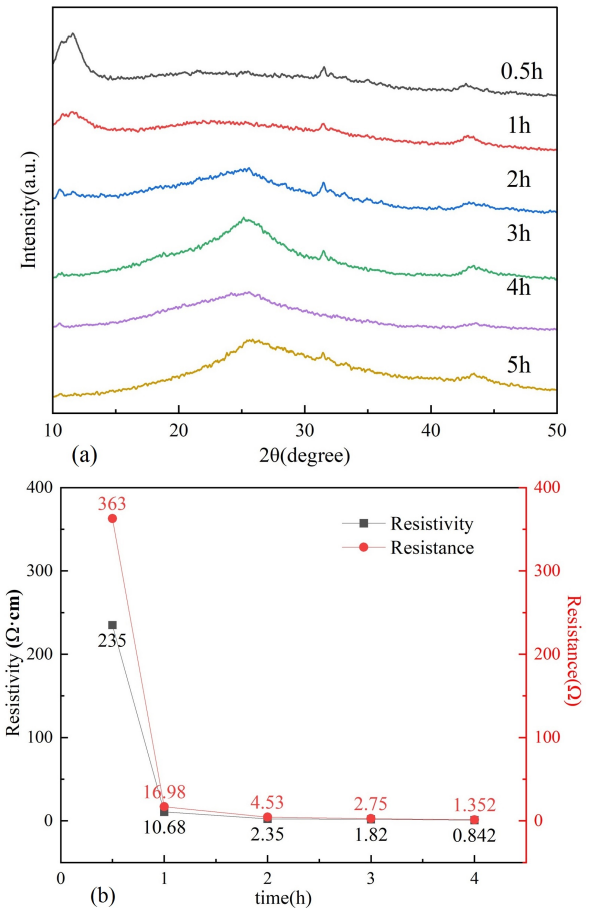

Figure 5. (a) XRD spectra and (b) Conductivity of samples at different reaction times (Reaction condition: VC/GO mass ratio = 1, 100 °C.)

Fig. 5 (a), the characteristic peak of GO remained visible after 1 hour, indicating an incomplete reaction from GO to rGO. Fig. 5 (b) showed that the resistivity was 10.68 Ω·cm, and the resistance was 16.98 Ω after 1 hour, higher than those observed at longer reaction times. The reaction appeared more complete after 2 hours, with a corresponding decrease in resistivity, highlighting the importance of adequate reaction time for full conversion and improved conductivity. As the reaction time extended, resistivity and resistance gradually decreased. This was because graphene oxide (GO) produces unsaturated conjugated carbon atoms during the reduction process. As shown in Fig. 5 (b), the characteristic peaks of rGO in the XRD pattern shifted progressively to the right with longer reaction times, indicating that the newly formed carbon atoms increased the surface defects, which made the surface active sites increase, thus providing more electron transport channels and reducing the obstacles to electron transmission [28].

3.3 Reaction temperature

The effect of reaction temperature on the preparation of rGO from GO using VC, and its impact on the crystal structure and conductivity were illustrated in Fig. 6. In Fig. 6 (a), only the characteristic peak of GO was present at 11°, which was observed when the reaction temperature reached 60 °C. This was consistent with the data in Fig. 6 (b), where the sample's resistivity at 60 °C was 55700 Ω·cm and the resistance was 79000 Ω. Compared to the results in Fig. 4 (c), this indicated that the reduction of graphene oxide at 60 °C was not ideal.

At 80 °C, the XRD spectrum showed characteristic peaks for both GO and RGO. The resistivity at 80 °C was 6.33 Ω·cm and the resistance was 7.21 Ω, with a d-spacing of 0.713 nm, suggested that a small amount of GO remained, leading to a higher resistivity compared to other temperatures. The mechanism for the chemical reduction of GO can be speculated as two-step S_N2 nucleophilic reactions followed by a thermal elimination stepidic reducing agent [20], the nucleophilicity of VC depended on its degree of ionization. Increasing the temperature accelerated the ionization of the VC solution and the thermal elimination process, facilitating the reaction with the epoxy, carbonyl, and carboxyl functional groups on the GO surface. At 100 °C, the XRD pattern showed the disappearance of the GO characteristic peak, indicating a complete reduction. The resistivity and resistance reached the lowest values of 1.82 Ω·cm and 2.75 Ω, respectively, indicating optimal reduction and improved conductivity. This highlighted the importance of an appropriate temperature was crucial for effective reduction and achieving the desired properties of rGO.

When the temperature exceeded 100 °C, the XRD spectrum showed only the characteristic peak of RGO, with a d-spacing of approximately 0.35 nm, indicating a more complete reaction. The resistivity tended to decrease slowly beyond this point. Therefore, it can be concluded that under

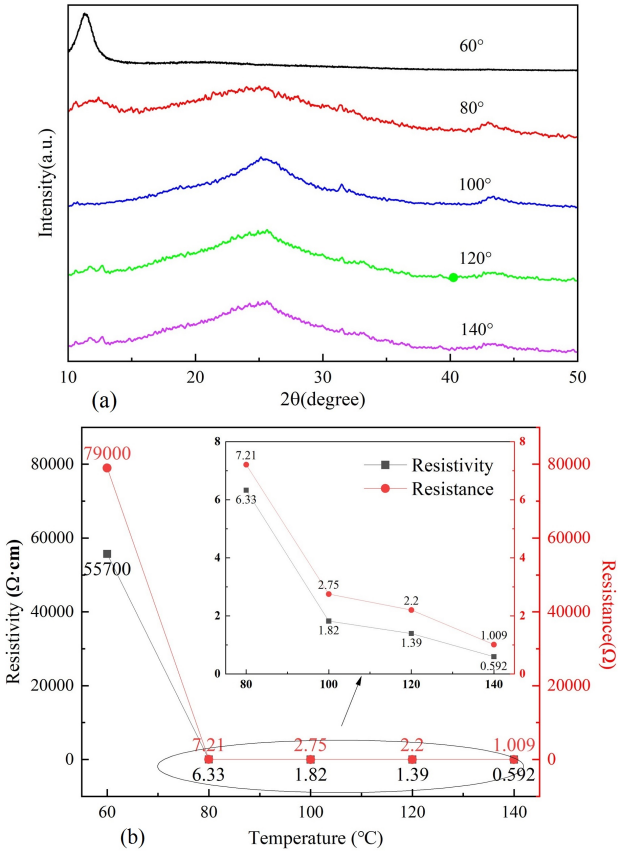

Figure 6. (a) XRD spectra and (b) Conductivity of samples at different reaction temperature (Reaction condition: VC/GO mass ratio = 1,44 h.)

the conditions of a VC/GO mass ratio of 1 and a reaction time of 4 hours, the optimal temperature for the reaction was 100 °C. This temperature ensured the most efficient reduction of GO to RGO, resulting in the lowest resistivity and highest conductivity of the synthesized material.

3.4 Material characterization

As shown in Fig. 7, within the wavenumber range of $3100-3600\ cm^{-1}$, the observed peaks were attributed to O-H stretching vibrations caused by adsorbed water molecules in the samples. For GO, the characteristic peaks at 1732 cm^{-1} (C=O), 1377 cm^{-1} (C-OH), and 1062 cm^{-1} (C-O) corresponded to carboxylic acid and carbonyl groups [29]. The aromatic C=C stretching vibration appeared at 1624 cm^{-1} [15]. The disappearance of these peaks in rGO confirmed that GO was effectively reduced. Compared to GO, the vibration peak of the C=O bond at 1724 cm^{-1} almost completely vanished after reduction, indicating that the C=O bonds on the surface of GO had been fully reduced. The significant decrease in peaks at 1375 cm^{-1} and 1061 cm^{-1} indicated that most oxygen-containing functional groups in GO had been reduced. This observation aligned with the XRD analysis results. The peak at 1541 cm^{-1} [11], attributed to the in-plane vibration of the C=C skeleton and adsorbed phytochemicals, primarily the carboxylate moieties of VC, were not observed for GO. According to previous literature and FTIR analysis, the hydroxyl and epoxide groups on the basal planes of the GO sheets were removed through a reaction with hydrogen atoms from vitamin C (S_N2 nucleophilic attack) [30].

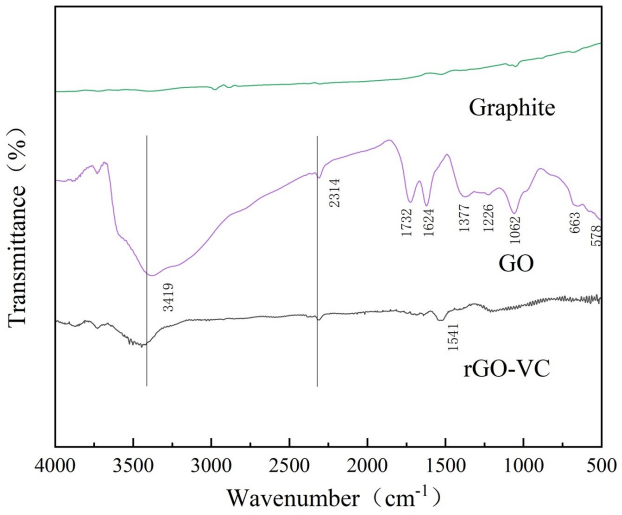

Figure 7. FT-IR spectra of different samples.

As shown in Fig. 8, the isotherm curves conformed to type IV isotherms, indicating that rGO had a porous structure. The specific surface area of rGO reduced by VC was 36.88 m^2/g, with an average pore diameter of 14.98 nm, indicating that the sample exhibited mesoporous characteristics. The gradual stabilization of the curve represents the behaviour of an H3-type hysteresis loop. The absence of a distinct saturation adsorption platform on the isotherm suggested irregular pore structures. Typically, the H3-type hysteresis loop described pore structures that included plate-like slits,

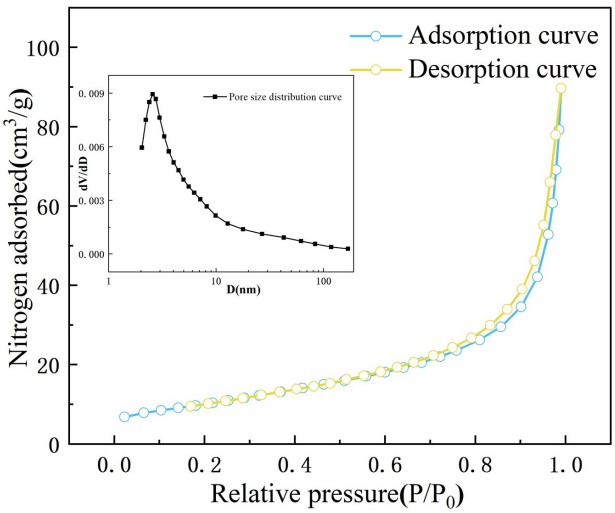

Figure 8. Nitrogen adsorption/desorption isotherms and pore size distribution curves of Samples(Reaction condition: VC/GO mass ratio = 1:1, 100 °C, 4 h).

cracks, and wedge-shaped pores. H3-type hysteresis loops were usually triggered by lamellar particle materials or fissure pore materials. This characteristic implied that the rGO synthesized in this study had a unique and complex porous structure, enhancing its potential applications in various fields such as adsorption, catalysis, and energy storage.

Fig. 9 (a) showed that GO aggregated into a cluster structure without significant layer separation, indicating strong interlayer interactions and poor exfoliation of the GO layers. In contrast, Fig. 9 (b) depicted the sample reduced using VC, where the sample exhibited uneven lamellar structures with noticeable edges, indicating the presence of multiple layers. The oxidized form of ascorbic acid might form $\pi-\pi$ stacking interactions between rGO sheets, thereby preventing agglomeration [31]. Moreover, rGO displayed an extensive irregularly shaped pore network structure, connected by folded nanosheets. This interconnected porous network can enhance the material's surface area and accessibility, making it suitable for applications in sensors, catalysis, and energy storage.

4. Conclusion

In this study, rGO was successfully synthesized from GO using VC as the reducing agent through a one-step hydrothermal method. VC effectively reduced the functional groups on the GO surface, forming C=C bonds. At VC/GO mass ratio of 0.5, there was a significant reduction in resistivity and electrical resistance. However, further increases in the VC/GO mass ratio resulted in minimal changes in conductivity while the d-spacing increased. An increase in reaction temperature enhanced the ionization and decomposition of VC, thereby improving reaction efficiency. Below 100 °C, the prepared samples still exhibited the characteristic GO structure. A porous network structure of the reduced rGO with an irregular shape was observed, which was interconnected by wrinkled nanosheets. Optimal conditions were observed at a VC/GO mass ratio of 1:1, a reaction temperature of 100 °C, and

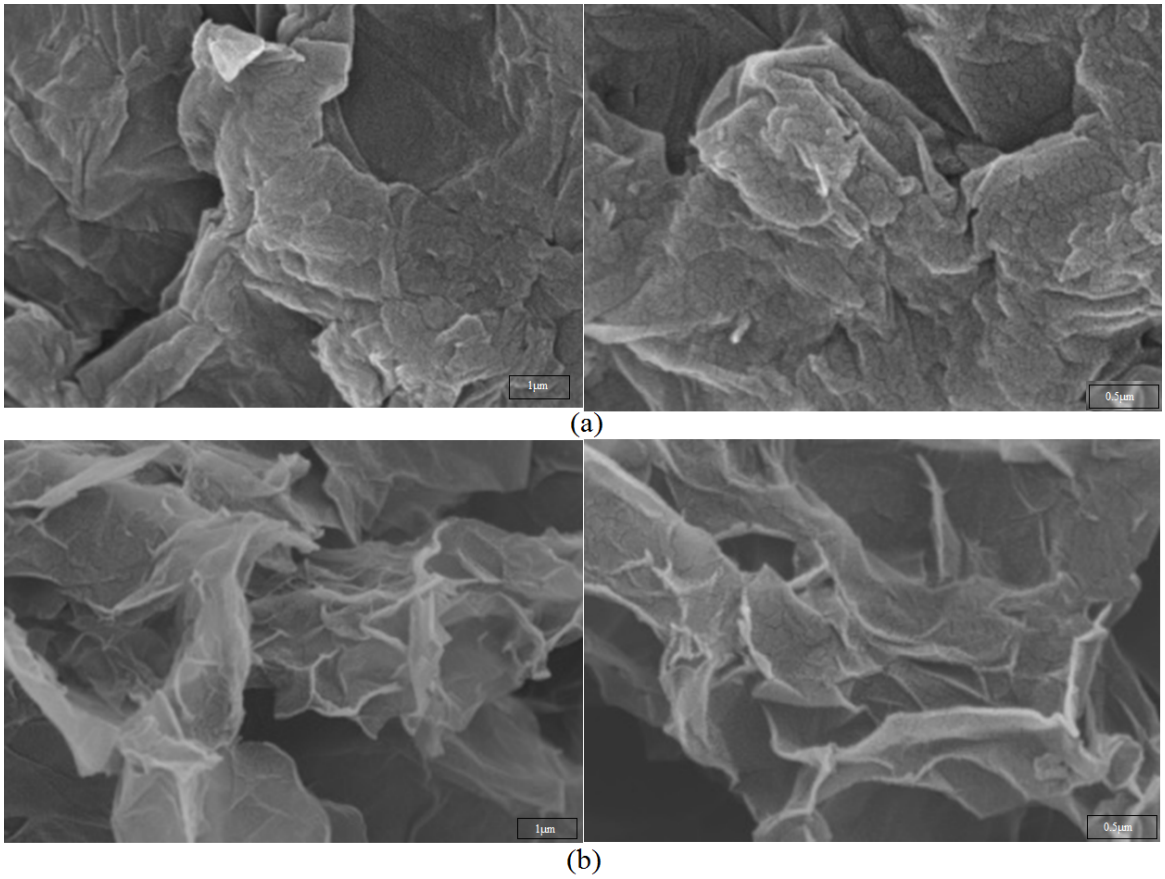

Figure 9. SEM images of samples (a)GO, (b) VC (Reaction condition: VC/GO mass ratio = 1:1, 100 °C, 4 h)

a reaction time of 3 hours. Under these conditions, the synthesized graphene material achieved a resistivity of 1.82 Ω·cm, a resistance of 2.75 Ω, and a specific surface area of 36.88 m^2/g, indicating its suitability as an excellent electrode material.

Acknowledgment
This work was supported by University Tun Hussein Onn Malaysia (UTHM) through a Multidisciplinary Research Grant (MDR) (Q708) and the Science and Technology Program of Liming Vocational University (LT202103). The author gratefully acknowledges Lai Mingrui, Jiang Wenhong, and SyYi Sim. for their work on the original version of this document.

Funding
Multidisciplinary Research Grant (MDR) (Q708) and Science and Technology Program of Liming Vocational University (LT202103).

Authors contributions
Authors have contributed equally in preparing and writing the manuscript.

Availability of data and materials
The data that support the findings of this study are available from the corresponding author upon reasonable request.

Conflict of interests
The authors declare that they have no known competing financial interests or personal relationships that could have appeared to influence the work reported in this paper.

References

[1] A. Ahmed, A. Singh, S. J. Young, V. Gupta, M. Singh, and S. Arya. "**Synthesis Techniques and Advances in Sensing Applications of Reduced Graphene Oxide (RGO) Composites: A Review**.". 165: 107373, 2022.
DOI: https://doi.org/10.1016/j.compositesa.2022.107373.

[2] A. M. Dimiev and J. M. Tour. "**Mechanism of Graphene Oxide Formation**.". *ACS Nano*, 8(3):3060–3068, 2014.
DOI: https://doi.org/10.1021/nn500606a.

[3] M. Buzaglo, M. Shtein, S. Kober, R. Lovrinčic, A. Vilan, and O. Regev. "**Critical Parameters in Exfoliating Graphite into Graphene**.". *Physical Chemistry Chemical Physics*, 15(12):4428–4435, 2013.
DOI: https://doi.org/10.1039/C3CP43205J.

[4] R. Castaldo, R. Avolio, M. Cocca, M. E. Errico, M. Lavorgna, J. Šalplachta, C. Santillo, and G. Gentile. "**Hierarchically Porous Hydrogels and Aerogels Based on Reduced Graphene Oxide, Montmorillonite and Hyper-Crosslinked Resins for Water and Air Remediation**.". *Chemical Engineering Journal*, 430:133162, 2022.
DOI: https://doi.org/10.1016/j.cej.2021.133162.

[5] D. Chen, L. Li, and L. Guo. "**An Environment-Friendly Preparation of Reduced Graphene Oxide Nanosheets via Amino Acid**.". *Nanotechnology*, 22(32):325601, 2011.
DOI: https://doi.org/10.1088/0957-4484/22/32/325601.

[6] P. Das, B. Mandal, and S. Gumma. "**Engineering of Structural and Surface Functional Characteristics of Graphite Oxide Nanosheets by Controlling Oxidation Temperature**.". *Applied Surface Science*, 504:144444, 2020.
DOI: https://doi.org/10.1016/j.apsusc.2019.144444.

[7] Y. Fang, Y. Zhang, C. Miao, K. Zhu, Y. Chen, F. Du, J. Yin, K. Ye, K. Cheng, and J. Yan. "**MXene-derived defect-rich TiO_2@rGO as high-rate anodes for full Na ion batteries and capacitors**.". *Nano-Micro Letters*, 12:1–16, 2020.
DOI: https://doi.org/10.1007/s40820-020-00471-9.

[8] M. J. Fernández-Merino, L. Guardia, J. I. Paredes, S. Villar-Rodil, P. Solís-Fernández, A. Martínez-Alonso, and J. M. D. Tascón. "**Vitamin C is an ideal substitute for hydrazine in the reduction of graphene oxide suspensions**.". *Journal of Physical Chemistry C*, 114(14):6426–6432, 2010.
DOI: https://doi.org/10.1021/jp100603h.

[9] J. Gao, F. Liu, Y. Liu, N. Ma, Z. Wang, and X. Zhang. "**Environment-friendly method to produce graphene that employs vitamin C and amino acid**.". *Chemistry of Materials*, 22(7):2213–2218, 2010.
DOI: https://doi.org/10.1021/cm902635j.

[10] M. Ikram, M. A. Bari, M. Bilal, F. Jamal, W. Nabgan, J. Haider, A. Haider, G. Nazir, A. D. Khan, K. Khan, A. K. Tareen, Q. Khan, G. Ali, M. Imran, E. Caffrey, and M. Maqbool. "**Innovations in the synthesis of graphene nanostructures for bio and gas sensors**.". *Biomaterials Advances*, 145:213234, 2022.
DOI: https://doi.org/10.1016/j.bioadv.2022.213234.

[11] R. Joshi, A. De Adhikari, A. Dey, and I. Lahiri. "**Green reduction of graphene oxide as a substitute of acidic reducing agents for supercapacitor applications**.". *Materials Science and Engineering: B*, 287:116128, 2023.
DOI: https://doi.org/10.1016/j.mseb.2022.116128.

[12] R. Kumar, W. Dias, R. J. G. Rubira, A. V. Alaferdov, A. R. Vaz, R. K.Singh, S. R. Teixeira, C. J. L. Constantino, and S. A. Moshkalev. "**Simple and fast approach for synthesis of reduced graphene oxide–MoS 2 hybrids for room temperature gas detection**.". *IEEE Transactions on Electron Devices*, 65(9):3943–3949, 2018.
DOI: https://doi.org/10.1109/TED.2018.2851955.

[13] R. Kumar, E. Joanni, W. K. Tan, and A. Matsuda. "**Microwave-aided ultra-fast synthesis of Fe_3O_4 nanoparticles attached reduced graphene oxide edges as electrode materials for supercapacitors,**.". *Materials Today Communications*, 38:108438, 2024.
DOI: https://doi.org/10.1016/j.mtcomm.2024.108438.

[14] R. Kumar and A. Kaur. "**Significantly Enhanced Photo Response of Hydrazine Hydrate Reduced Graphene Oxide Films Modified with Swift Heavy Ion Irradiation of Silver (Ag^{8+}) Ions**.". *Optical Materials*, 152:115528, 2024.
DOI: https://doi.org/10.1016/j.optmat.2024.115528.

[15] J. K. Lee, S. Lee, Y. I. Kim, J. G. Kim, B. K. Min, K. I. Lee, Y. Park, and P. John. "**The Seeded Growth of Graphene**.". *Scientific Reports*, 4:1–5, 2014.
DOI: https://doi.org/10.1038/srep05682.

[16] S. Liu, P. Wang, C. Liu, Y. Deng, S. Dou, Y. Liu, J. Xu, Y. Wang, W. Liu, and W. Hu. "**Nanomanufacturing of RGO-CNT hybrid film for flexible aqueous Al-ion batteries**.". *Small*, 16(37):2002856, 2020.
DOI: https://doi.org/10.1002/smll.202002856.

[17] A. Lundstedt, R. Papadakis, H. Li, Y. Han, K. Jorner, J. Bergman, K. Leifer, H. Grennberg, and H. Ottosson. "**White-Light Photoassisted Covalent Functionalization of Graphene Using 2-Propanol**.". *Small Methods*, 1(11):1700214, 2017.
DOI: https://doi.org/10.1002/smtd.201700214.

[18] F. Ma, F. Tang, B. Yang, Q. Guo, P. Li, and L. Yu. "**Vitamin C-Reduced Graphene Oxide/Fe_3O_4 Composite for Simultaneous Removal of Aflatoxin B1 and Benzo(a)Pyrene in Vegetable Oils**.". *LWT*, 203:116342, 2024.
DOI: https://doi.org/10.1016/j.lwt.2024.116342.

[19] D. R. Madhuri, K. Kavyashree, A. R. Lamani, H. S. Jayanna, G. Nagaraju, and S. Mundinamani. "**Reduction of Graphene Oxide by Phyllanthus Emblica as a Reducing Agent–A Green Approach for Supercapacitor Application**.". *Materials Today: Proceedings*, 49:865–869, 2021.
DOI: https://doi.org/10.1016/j.matpr.2021.06.173.

[20] F. Mindivan and M. Göktaş. "**Effects of various Vitamin C amounts on the green synthesis of reduced graphene oxide**.". *Materialpruefung/Materials Testing*, 61(10):1007–1011, 2019.
DOI: https://doi.org/10.3139/120.111416.

[21] B. B. Murphy, N. V. Apollo, P. Unegbu, T. Posey, N. Rodriguez-Perez, Q. Hendricks, F. Cimino, A. G. Richardson, and F. Vitale. "**Vitamin C-Reduced Graphene Oxide Improves the Performance and Stability of Multimodal Neural Microelectrodes**.". *Science*, 25(7):104652, 2022.
DOI: https://doi.org/10.1016/j.isci.2022.104652.

[22] S. Palanisamy, V. Velusamy, S. W. Chen, T. C. K. Yang, S. Balu, and C. E. Banks. "**Enhanced Reversible Redox Activity of Hemin on Cellulose Microfiber Integrated Reduced Graphene Oxide for H_2O_2 Biosensor Applications**.". *Carbohydrate Polymers*, 204: 152–160, 2018.
DOI: https://doi.org/10.1016/j.carbpol.2018.10.001.

[23] P. Rani, R. Dahiya, M. Bulla, R. Devi, K. Jeet, A. Jatrana, and V. Kumar. "**Hydrothermal-Assisted Green Synthesis of Reduced Graphene Oxide Nanosheets (RGO) Using Lemon (Citrus Limon) Peel Extract**.". *Materials Today: Proceedings*, 2023.
DOI: https://doi.org/10.1016/j.matpr.2023.04.419.

[24] I. A. Sahito, K. C. Sun, A. A. Arbab, and S. H. Jeong. "**Synergistic Effect of Thermal and Chemical Reduction of Graphene Oxide at the Counter Electrode on the Performance of Dye-Sensitized Solar Cells**.". *Solar Energy*, 190:112–118, 2019.
DOI: https://doi.org/10.1016/j.solener.2019.08.012.

[25] S. Sahoo, A. Milton, A. Sood, R. Kumar, S. Choi, C. K. Maity, and S. S. Han. "**Microwave-assisted synthesis of perovskite hydroxide-derived Co_3O_4/SnO_2/reduced graphene oxide nanocomposites for advanced hybrid supercapacitor devices**.". *Journal of Energy Storage*, 99:113321, 2024.
DOI: https://doi.org/10.1016/j.est.2024.113321.

[26] A. D. Sontakke, S. Tiwari, and M. K. Purkait. "**A Comprehensive Review on Graphene Oxide-Based Nanocarriers: Synthesis, Functionalization and Biomedical Applications**.". *FlatChem*, 38: 100484, 2023.
DOI: https://doi.org/10.1016/j.flatc.2023.100484.

[27] D. Tasis, K. Papagelis, P. Spiliopoulos, and C. Galiotis. "**Efficient Exfoliation of Graphene Sheets in Binary Solvents**.". *Materials Letters*, 94:47–50, 2013.
DOI: https://doi.org/10.1016/j.matlet.2012.12.027.

[28] L. Xian, R. You, J. Zhang, J. Wang, M. Ni, X. Zhang, S. Liu, Y. Zhang, and Y. Lu. "**Preparation of Urea-Modified Graphene Oxide-Gold Composite Detection of Nitrite**.". *Applied Surface Science*, page 152917, 2022.
DOI: https://doi.org/10.1016/j.apsusc.2022.152917.

[29] S. Yang, Z. Tao, Q. Kong, J. Li, X. Li, X. Yan, J. Liu, Y. Tong, and Z. Liu. "**Preparation of graphitic foil with high thermal conductivity using Vitamin C as reductant and binder**.". *Chemical Engineering Journal*, 473:145330, 2023.
DOI: https://doi.org/10.1016/j.cej.2023.145330.

[30] S. Zhang, H. Wang, J. Liu, and C. Bao. "**Measuring the Specific Surface Area of Monolayer Graphene Oxide in Water**.". *Materials Letters*, 261:127098, 2020.
DOI: https://doi.org/10.1016/j.matlet.2019.127098.

[31] Y. Zhang, L. Zhang, and C. Zhou. "**Review of Chemical Vapor Deposition of Graphene and Related Applications**.". *Accounts of Chemical Research*, 46(10):2329–2339, 2013.
DOI: https://doi.org/10.1021/ar300203n.